the plant journal

SEB SOCIETY FOR EXPERIMENTAL BIOLOGY

The Plant Journal (2024) doi: 10.1111/tpj.17030

Maximizing saffron apocarotenoid production in varied tomato fruit carotenoid contexts

Maria Lobato-Gómez[1], Margit Drapal[2], Rafael Fernández-Muñoz[3], Silvia Presa[1], Ana Espinosa[1], Paul D. Fraser[2], Lourdes Gómez-Gómez[4], Diego Orzaez[1] and Antonio Granell[1,*]

[1]*Instituto de Biología Molecular y Celular de Plantas, CSIC-Universidad Politécnica de València, Valencia 46022, Spain,*
[2]*School of Biological Sciences, Royal Holloway, University of London, Egham, Surrey TW20 0EX, UK,*
[3]*Instituto de Hortofruticultura Subtropical y Mediterránea, CSIC-Universidad de Málaga, Algarrobo Costa, Málaga 29750, Spain, and*
[4]*Instituto Botánico, Universidad de Castilla-La Mancha, Albacete 02006, Spain*

Received 13 May 2024; revised 23 July 2024; accepted 3 September 2024.
*For correspondence (e-mail agranell@ibmcp.upv.es)

SUMMARY

Saffron spice owes its commercial appreciation to its specific apocarotenoids: crocins, picrocrocin, and safranal. In *Crocus sativus*, these compounds are biosynthesized from zeaxanthin through oxidative cleavage by the carotenoid cleavage dioxygenase 2 (CCD2). Transgenic tomato plants expressing *CsCCD2* in the fruit, named Tomaffron, accumulate high levels of saffron apocarotenoids despite the low substrate availability for *Cs*CCD2. In the present study, *CsCCD2* has been introduced into Xantomato; this tomato variety accumulates high levels of zeaxanthin and β-carotene in ripe fruit due to a combination of four mutant alleles. Xantomato and Tomaffron genotypes have been combined to optimize apocarotenoid production. The best transgenic lines accumulated 15 and 14 times more crocins and picrocrocin than Tomaffron, alongside a fourfold increase in β-carotene compared to Xantomato, albeit at a cost in fruit yield. Segregation of the four mutations has been carried out to find the best combination for obtaining high levels of saffron apocarotenoids without adverse effects on fruit yield. Plants harboring the *high-pigmented 3* (*hp3*) and *BETA* (B^{Sh}) mutations accumulated 6 and 15 times more crocins and picrocrocin than Tomaffron, without observable pleiotropic effects. Additionally, those high levels of saffron apocarotenoids were obtained in fruit accumulating high levels of both lycopene and β-carotene independently or in combination, suggesting a regulatory role for the apocarotenoids produced and indicating that it is possible to increase the levels of both types of healthy promoting molecules simultaneously.

Keywords: saffron apocarotenoids, tomato, metabolic engineering, carotenoids.

INTRODUCTION

Saffron spice is derived from red stigmas of the *Crocus sativus* flower (Winterhalter & Straubinger, 2000), containing over 150 volatile and aromatic compounds, with less than a dozen of them contributing significantly to the distinctive color, bitter taste, and fragrance of saffron (Husaini, 2014). It takes 80 kg of flowers to yield 1 kg of saffron spice, rendering saffron the most valuable spice known (Rameshrad et al., 2018). For nearly 3000 years, saffron has been utilized for culinary, medicinal, and dying purposes (Bathaie et al., 2014; Rameshrad et al., 2018). Its applications extend to perfumes and cosmetics, while ongoing research delves into its potential medicinal properties (Hosseini et al., 2018). Several studies have highlighted antioxidant and anti-inflammatory attributes of saffron, demonstrating efficacy in leukemia, cardiovascular, digestive, ocular, and Alzheimer's diseases (Cerdá-Bernad et al., 2022).

Saffron apocarotenoid biosynthesis in the plastids of *C. sativus* flower stigma (Figure 1) begins with the oxidative cleavage of zeaxanthin at the 7,8 and 7′,8′ double bonds catalyzed by carotenoid cleavage dioxygenase 2 (*Cs*CCD2), resulting in 3-OH-β-cyclocitral (HTCC) and crocetin dialdehyde (Frusciante et al., 2014). Next, *Cs*ALDH3 catalyzes the conversion of crocetin dialdehyde into crocetin. Crocins, the main compounds contributing to the color of saffron, are then formed through crocetin glycosylation mediated by *Cs*UGT2 and *Cs*UGT91P3. *Cs*UGT709G1 converts HTCC into picrocrocin, which is further converted during spice processing into safranal, the primary

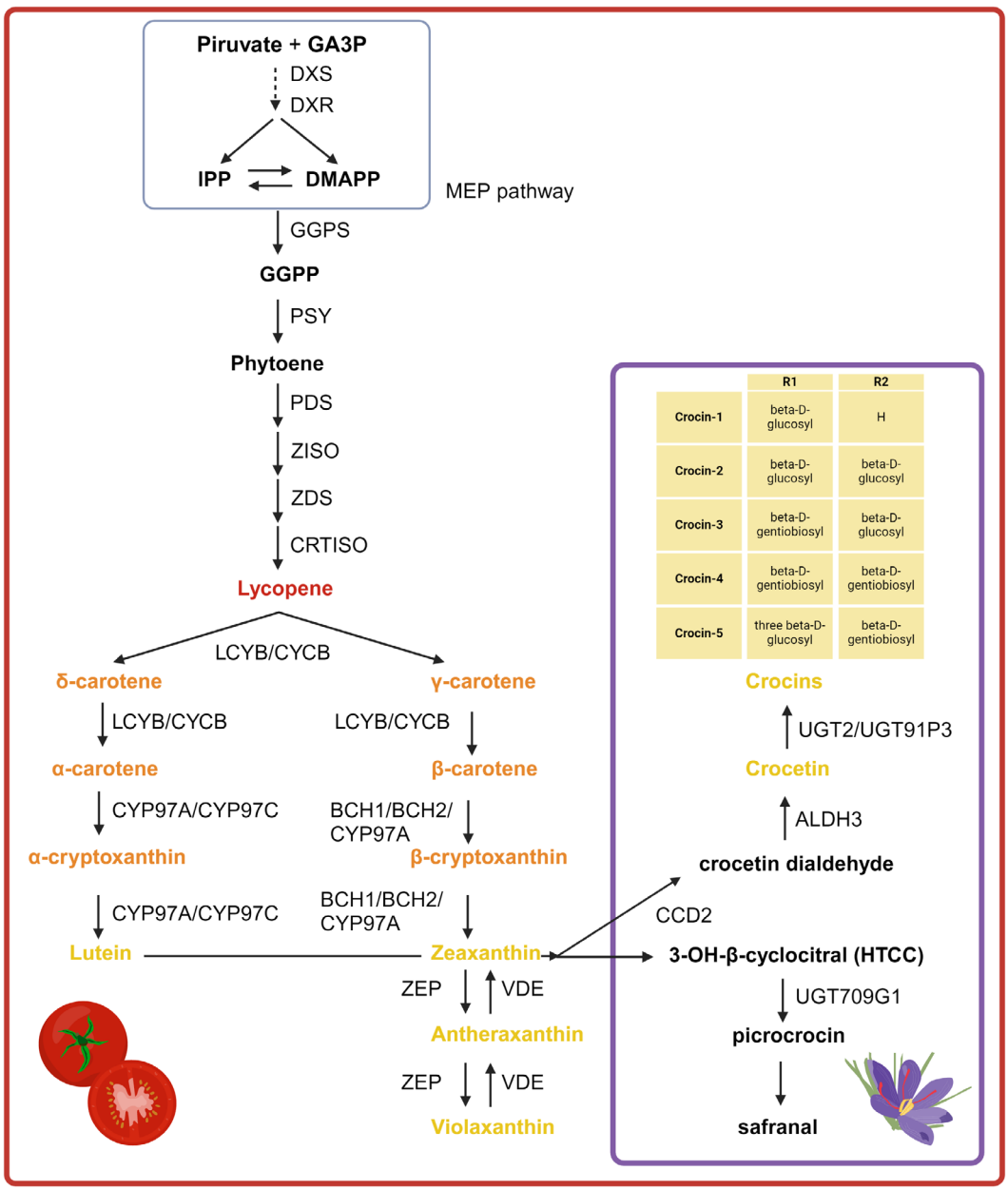

Figure 1. Carotenoid and saffron apocarotenoid biosynthesis. ALDH, aldehyde dehydrogenase; BCH, β-carotene hydroxylase; CCD, carotenoid cleavage dioxygenase; CRTISO, carotenoid isomerase; CYCB, lycopene β-cyclase (chromoplast isoform); CYP97, carotene –hydroxylase; DMAPP, dimethylallyl pyrophosphate; DXS, deoxy xylulose phosphate synthase; DXR, deoxy xylulose phosphate reductoisomerase; GA3P, glyceraldehyde 3-phosphate; GGPP, geranyl geranyl diphosphate; IPP, isopentenyl pyrophosphate; LYCB, lycopene β-cyclase (chloroplast isoform); LYCE, lycopene ε-cyclase; PDS, phytoene desaturase; PSY, phytoene synthase; UGT, UDP-glucuronosyltransferase; VDE, violaxanthin de-epoxidase; ZDS, ζ-carotene desaturase; ZEP, zeaxanthin epoxidase; ZISO, ζ-carotene isomerase. Adapted from (Hirschberg, 2001; López et al., 2021; Moraga et al., 2004; Rodriguez-Concepcion et al., 2018).

responsible for the aroma of saffron (López et al., 2021; Moraga et al., 2004).

Apocarotenoids of saffron are also synthesized in *Buddelja davidi* (Ahrazem et al., 2017), *Gardenia jasminoides* (Xu et al., 2020), *Crocus ancyrensis* (Ahrazem et al., 2016), and *Verbascum* species (Morote, Rubio-Moraga, et al., 2023). The CCDs identified in these species have been proven to use zeaxanthin as a substrate *in vitro* or by producing saffron apocarotenoids in heterologous platforms. The CCD4a and CCD4-1 enzymes from *G. jasminoides* and *V. giganteum* can also utilize β-carotene as a substrate. In the case of *Gj*CCD4a, the use of lycopene as a substrate has also been reported (Morote, Rubio-Moraga, et al., 2023; Xu et al., 2020; Zheng et al., 2022).

There is significant interest in producing saffron apocarotenoids in heterologous platforms due to their biological properties, which contrast with the high cost and low sustainability of saffron spice production. The knowledge of CCDs with the specific capabilities to cleave zeaxanthin has enabled the generation of saffron apocarotenoids in various plant heterologous platforms (Ahrazem et al., 2016, 2017; Frusciante et al., 2014; Xu et al., 2020). Crocetin was generated in maize endosperm by transiently expressing *CsCCD2* (Frusciante et al., 2014). Crocins were obtained in *Nicotiana tabacum*, *N. glauca*, and rice callus (Ahrazem et al., 2016) by stable transformation of *CsCCD2* (Ahrazem, Zhu, et al., 2022; Huang et al., 2022). Crocins and picrocrocin have been produced in *N. benthamiana* leaves through transient expression of *CsCCD2* (Demurtas et al., 2023; Martí et al., 2020), *GjCCD4a* (Zheng et al., 2022), and *VgCCD4-1* (Morote, Rubio-Moraga, et al., 2023) and in citrus callus expressing *GjCCD4a* (Zheng et al., 2022). Crocins, picrocrocin, and safranal were successfully produced through *CsCCD2* overexpression transiently in *N. benthamiana* (Martí et al., 2020), in transgenic potato tuber (Gómez Gómez et al., 2022), and tomato fruit (Ahrazem, Diretto, et al., 2022; Frusciante et al., 2022; Morote, Lobato-Gómez, et al., 2023). Among these platforms, *CsCCD2* transgenic tomato fruits, named Tomaffron (TF), showed the highest accumulation levels of saffron apocarotenoids. This is not surprising since tomato fruit is an excellent biofactory for added-value metabolites because it is a sink organ whose developmental program during ripening is directed to accumulating specialized metabolites. These metabolites can be purified, consumed in fresh fruit, or stored in processed tomato products (Li et al., 2018). Apart from saffron apocarotenoids, anthocyanins (Butelli et al., 2008), betalains (Polturak et al., 2017), and ketocarotenoids (Nogueira et al., 2017) have been produced in tomato fruit using biotechnology approaches.

Although the preferred substrates of *Cs*CCD2 enzyme appear to be zeaxanthin and lutein (Frusciante et al., 2014; Ahrazem, Diretto, *et al.*, 2022), the tomato cultivar employed to this date as chassis to engineer apocarotenoid production (*Solanum lycopersicum* cv. MoneyMaker (MM)) accumulates, instead, mostly lycopene and, to a lesser extent, β-carotene (Ahrazem, Diretto, et al., 2022) in the ripe fruit. Theoretically, this leaves room for improvement of the background genetics of the tomato apocarotenoid biofactory through a dedicated optimization of the carotenoid biosynthetic pathway.

The carotenoid biosynthetic pathway in plants has been intensely studied (Hirschberg, 2001; Rodriguez-Concepcion et al., 2018) and is represented in Figure 1. Several natural mutations (Chattopadhyay et al., 2021) and transgenic (Fraser et al., 2009) approaches have been reported to alter the carotenoid biosynthetic pathway in tomato fruit. The transgenic biofortification of zeaxanthin has been pursued (D'Ambrosio et al., 2011; Karniel et al., 2020), but the highest reported levels of zeaxanthin accumulation in fruit resulted from stacking four mutations in a variety termed Xantomato (Karniel et al., 2020). The *BETA* mutation in the CYCB from wild tomato *Solanum habrochaites*, named B^{Sh}, increased β-carotene content in the fruit from 5–10% to 45–50% (Ronen et al., 2000). When B^{Sh} is combined with the recessive *high-pigmented 2 dark green* ($hp2^{dg}$), (Levin et al., 2003), *high-pigmented 3* (*hp3*) (Galpaz et al., 2008) and *green stripe* (*gs*) mutations resulted in tomato fruits with high accumulation of β--carotene and zeaxanthin. However, these mutations have a pleiotropic negative effect on plant growth and stress tolerance (Karniel et al., 2020).

In this work, we aimed to maximize the production of saffron apocarotenoids in tomato fruit by engineering and genetic crossing strategies to incorporate *Cs*CCD2 in different carotenoid backgrounds in the fruit to evaluate the effect on carotenoids and saffron apocarotenoids. The final aim is to elucidate the best combination of mutations that optimize healthy compound production while avoiding adverse effects on plant yield.

RESULTS

Accumulation of high levels of crocins, picrocrocin, and β-carotene in fruits of transgenic Xantomato plants expressing *CsCCD2*

A Xantomato line (Karniel et al., 2020) with high zeaxanthin levels in ripe fruits was used to test if higher levels of this carotenoid in tomato result in enhanced levels of saffron apocarotenoid accumulation in *Cs*CCD2-expressing transgenic tomatoes. For this purpose, Xantomato cotyledons were transformed with the saffron cassette. High production of non-organogenic vitreous calli was developed in selective media, making the process significantly slower and less efficient in this line compared to other tomato cultivars (data not shown). Nevertheless, a total of seven T0 plants (termed Xantoffron) were confirmed by PCR for *Cs*CCD2 presence and transferred to soil. Both wild-type and transgenic Xantomato showed compromised growth in our greenhouse conditions. Four transgenic plants reached the flowering stage, and two lines (1A and 9) produced fruits with seeds. Both T0 lines expressed *Cs*CCD2 and accumulated crocins and picrocrocin at different levels and showed an altered carotenoid profile compared to Xantomato (Figure S1).

Very few T1 seeds were obtained from both T0 lines, and the germination rate was comparatively low (5%). Only two and three T1 plants from lines 1A and 9 could grow and showed a compromised growth in the greenhouse, with a high flower abortion rate and a shallow fruit set. Fruits from the different plants from the same line were mixed to have enough material.

The T1 fruits from both transgenic lines showed an altered phenotype compared to Xantomato; their inner fruit color was more orange than the yellow of Xantomato (Figure 2A). Xantoffron 1A exhibited a much higher *CsCCD2* expression in the fruit than line 9 (x1800 fold) (Figure 2B) and produced approx. 15 times more crocins than Tomaffron (TF). In contrast, Xantoffron 9 produced seven times less crocins than TF (Figure 2C). Similarly to crocins, Xantoffron 1A produced 14 times more picrocrocin and HTCC than TF, and Xantoffron 9 produced only 1.5 times more picrocrocin and HTCC than TF (Figure 2D). These results indicate that levels of zeaxanthin were the most critical limiting factor for high levels of saffron apocarotenoids in TF.

Interestingly, fruits from Xantoffron lines showed an altered carotenoid profile compared to the parent Xantomato line (Figure 2E). Zeaxanthin and lutein were not detected in Xantoffron 1A, strongly supporting their conversion by the engineered *CsCCD2*. Consistent with the much lower expression of *CsCCD2* in line 9, zeaxanthin levels were reduced; however, half of the zeaxanthin content detected in Xantomato was retained, while lutein levels were like those in Xantomato (Figure 2F).

Strikingly, total carotenoid levels increased in the engineered fruits. In the T1 fruits, β-carotene levels were almost 4 and 3 times higher in Xantoffron 1A and 9, respectively, than in control Xantomato. Phytoene and lycopene reached significantly high levels in both transgenic lines, increasing 100 (line 1A) and 10-fold (line 9) compared to Xantomato. The tomato fruit carotenoid pathway seems to respond to our heterologous *Cs*CCD2 engineering with a change in the carotenoid profile in a dose-dependent manner.

To better understand the effect our engineering approach may have on the endogenous carotenoid pathway in the ripe fruit, the expression of some MEP and carotenoid biosynthetic pathway genes was determined in fruits from T1 lines. The gene expression results on Xantoffron 1A and 9 fruits revealed that carotenoid biosynthesis was boosted at different points to impact β-carotene accumulation: the MEP pathway and lycopene to β-carotene conversion were up-regulated. In contrast, β-carotene conversion to zeaxanthin was downregulated (Figure 2G).

As in T0, very few T2 seeds were obtained from these lines, and only two plants from each line could develop properly. Unfortunately, no viable fruit was set, and both transgenic lines were lost. Overall, using Xantomato as a starting material for our engineering approach harbors several disadvantages regarding plant viability.

Carotenoid mutations in Xantomato have an effect on saffron apocarotenoid accumulation in a heterozygous state

The four carotenoid-related mutations in Xantomato resulted in high levels of crocin and picrocrocin accumulation in fruit and plants with poor yields and compromised growth. To overcome this problem and to learn more about its genetic basis, we crossed Xantomato with TF to obtain different combinations of the Xantomato mutations with *CsCCD2*. Also, a population of F1 hybrids with *hp3*/B^{Sh}, an intermediate mutant carrying only two Xantomato mutations, was produced. The idea was to elucidate the best carotenoid gene combination to maximize saffron apocarotenoid accumulation and fruit yield.

The F1 plants from both crosses showed a vegetative phenotype similar to TF plants. In contrast, fruits from the cross with Xantomato or *hp3*/B^{Sh} with TF accumulated three or twice the amount of crocins compared to TF (Figure 3A). The accumulation of picrocrocin and HTCC also increased significantly in the F1 fruits from both Xantomato or *hp3*/B^{Sh} crosses, with an increase of 6 and 3 times compared to TF (Figure 3B). The F1 fruits showed an outer skin with a darker color with changed color parameters (Figure 4C). Consistent with the increase in crocin accumulation, the inner part of the fruit showed a more intense yellow color than TF (Figure 4D).

Significant changes in carotenoid accumulation and compositions were also observed (Figure 3C; Table S3). In contrast to their parental lines, TF and F1 fruits from both crosses failed to accumulate lutein and zeaxanthin, suggesting that *Cs*CCD2 activity has consumed both carotenoids. Interestingly, the Xantomato x TF cross F1 fruits accumulated more carotenoids than both parentals. (Figure 3D). Furthermore, the composition of carotenoids in these F1 fruits changed relative to their carotenoid mutant parental lines. While in Xantomato and *hp3*/B^{Sh} phytoene and lycopene were detected at low levels, in the F1 fruits from both crosses, the content of these carotenoids increased significantly, with a higher accumulation observed in F1 fruits from the Xantomato cross. In addition, the β-carotene content was substantially higher in the F1 fruits than in TF (Table S3).

Figure 2. Results of T1 fruits from transgenic Xantomato. (A) Phenotype of fruits. Scale bar: 2.5 cm. (B) *CsCCD2* expression (C) Relative crocin accumulation, quantified via LC–MS and normalized with genistein as internal standard (IS). (D) Relative picrocrocin and HTCC accumulation, quantified via LC–MS and normalized with genistein as IS. (E) Relative carotenoid accumulation, quantified via HPLC-PDA and normalized with canthaxanthin as IS. Line grouping is based on an ANOVA test for *CsCCD2* expression, total crocin, picrocrocin, HTCC, or carotenoid content, followed by a Tukey post-hoc test. Error bars represent the SD of biological replicates (n = 3). (F) Relative accumulation of individual carotenoids, quantified via HPLC-PDA and normalized with canthaxanthin as IS. Line grouping based on an ANOVA test for each carotenoid content, followed by a Tukey post-hoc test. (G) Relative expression of MEP and carotenoid pathway genes, using Xantomato as the reference line.

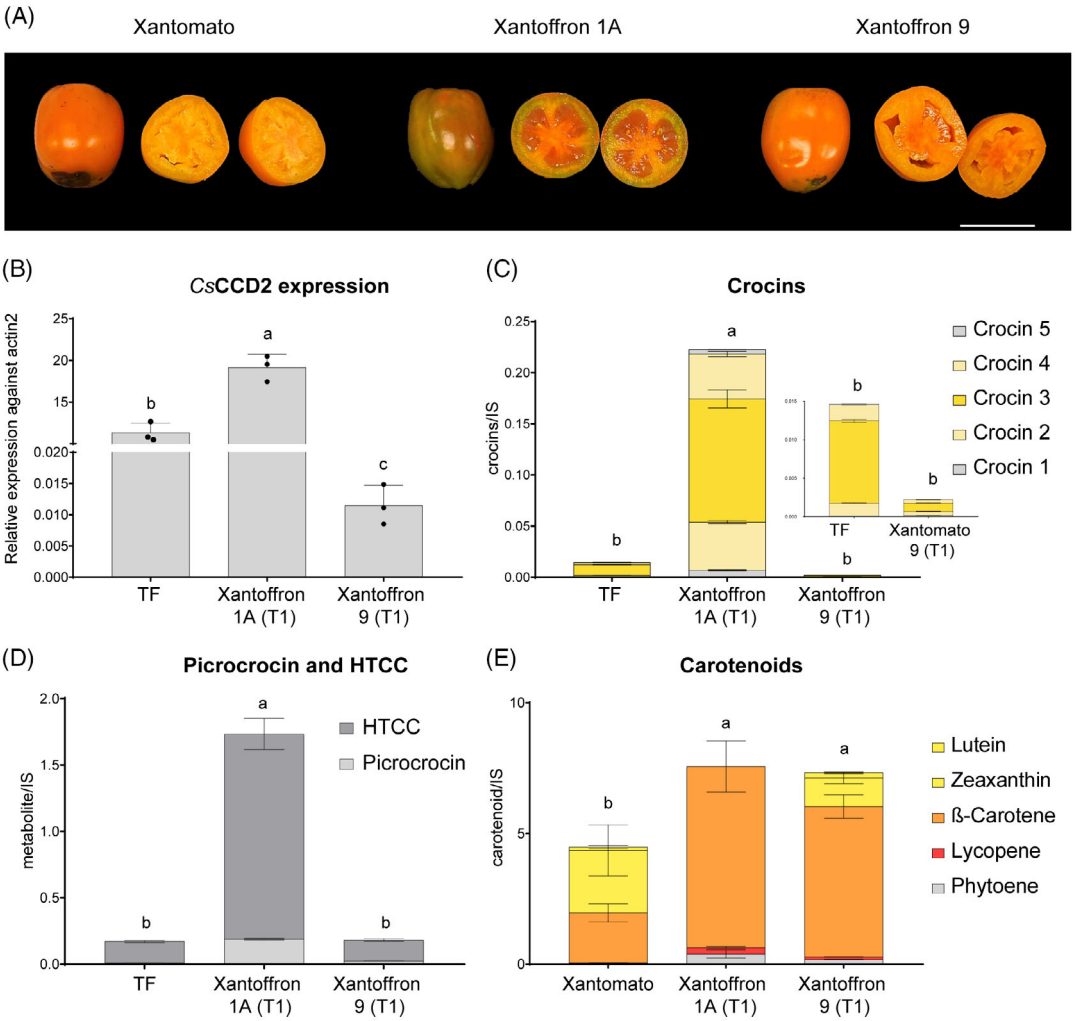

(F) **Individual carotenoid relative quantification (carotenoid/IS)**

Line	Phytoene	Lycopene	β-carotene	Zeaxanthin	Lutein
Xantomato	0.038 ± 0.009 **b**	0.009 ± 0.009 **b**	1.913 ± 0.346 **b**	2.394 ± 0.977 **a**	0.199 ± 0.200 **a**
Xantoffron 1A (T1)	0.390 ± 0.162 **a**	0.948 ± 0.351 **a**	7.184 ± 1.012 **a**	0 **b**	0 **b**
Xantoffron 9 (T1)	0.173 ± 0.011 **ab**	0.367 ± 0.045 **b**	5.958 ± 0.480 **a**	1.096 ± 0.214 **ab**	0.127 ± 0.037 **a**

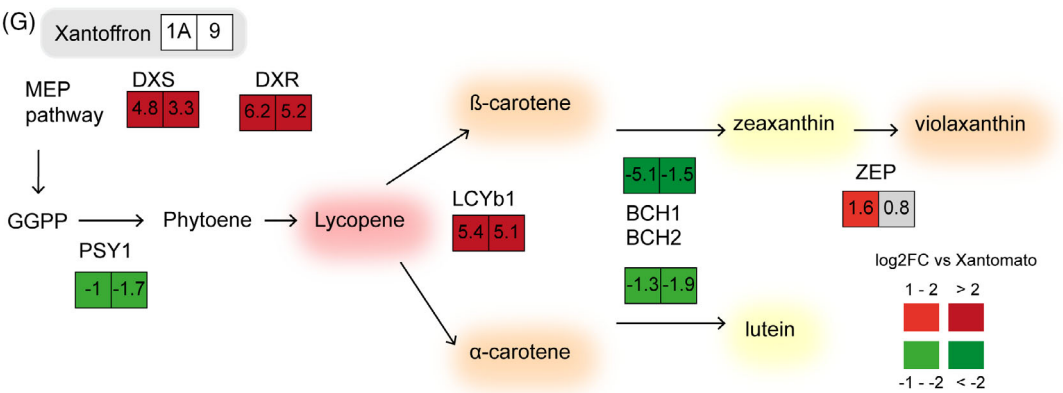

The Plant Journal published by Society for Experimental Biology and John Wiley & Sons Ltd.,
The Plant Journal, (2024), doi: 10.1111/tpj.17030

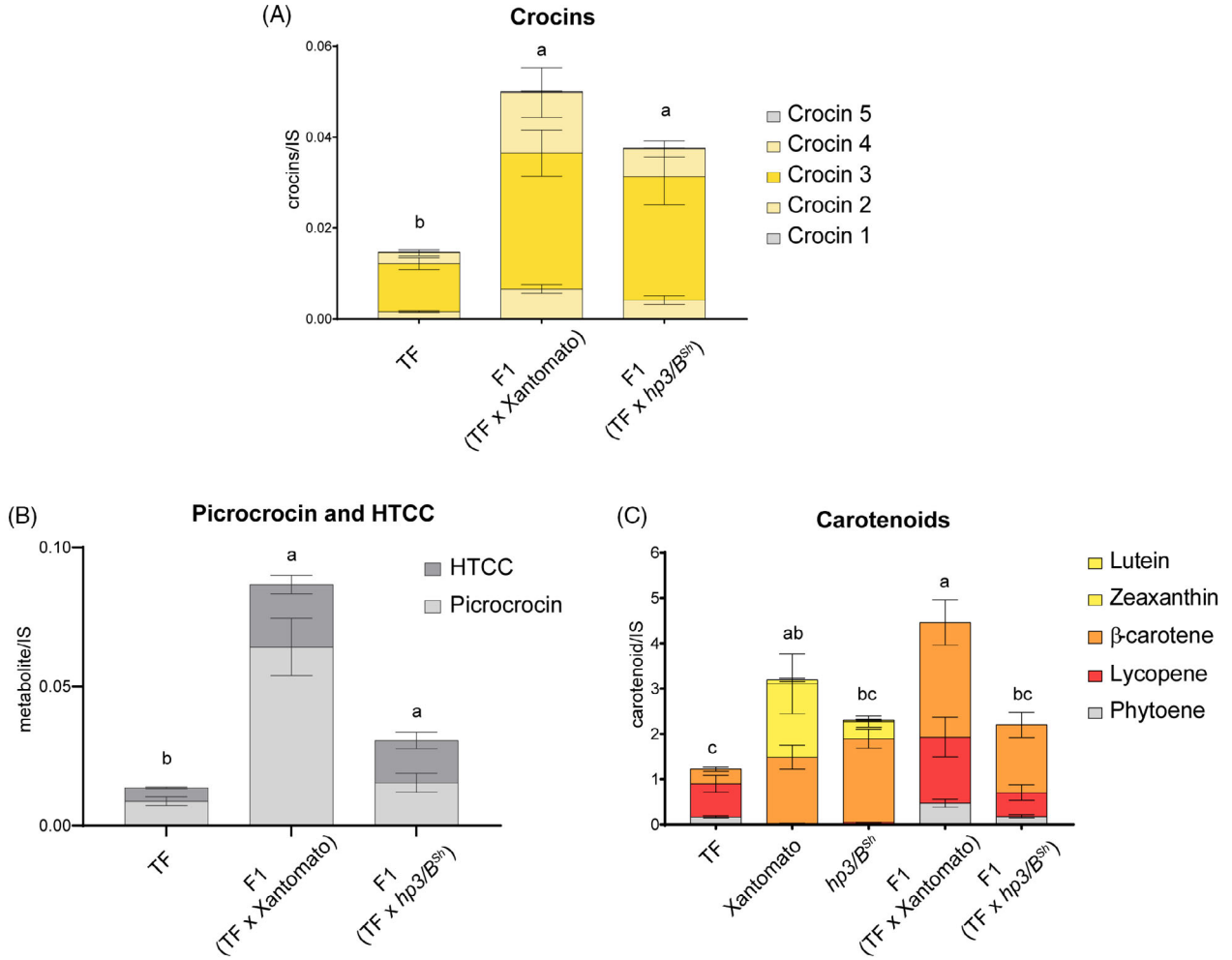

Figure 3. Results of F1 fruits from the cross of Xantomato with TF. (A) Relative crocin accumulation, quantified via LC–MS and normalized with genistein as internal standard (IS). (B) Relative picrocrocin and HTCC accumulation, quantified via LC–MS and normalized with genistein as IS. (C) Relative carotenoid accumulation, quantified via HPLC-PDA and normalized with canthaxanthin as IS. Line grouping is based on an ANOVA test for total metabolite content in each graph, followed by a Tukey post-hoc test. Error bars represent the SD of biological replicates (n = 3).

These results show that the *hp3* and B^{Sh} mutations in a heterozygous state already have a positive effect on both saffron apocarotenoid and carotenoid accumulation, while the two extra mutations of Xantomato ($hp2^{dg}$ and *gs*) in heterozygosis boost these effects.

Effect of different combinations of carotenoid mutations on saffron apocarotenoid production in *Cs*CCD2-engineered tomatoes

96 F2 plantlets derived from the cross of TF with Xantomato were germinated on hygromycin and screened for the presence of the mutations. From this pool, 28 plants were selected and transferred to soil (Table S4). Nine plants did not survive the greenhouse conditions, and another eight did not produce fruits. The numerous plant losses indicate that these mutations produce pleiotropic effects that compromise plant fertility (Karniel et al., 2020). The F2 plants that made it to produce fruits and the subsequent F3 plants used in this study, together with the phenotyping results for *gs*, are indicated in Figure 4A,B.

The population was first assessed using the outer fruit color parameters. Results showed that fruits clustered based on the genotype for the B^{Sh} mutation; plants harboring both alleles from MM showed a redder outer fruit color. Conversely, plants harboring the B^{Sh} mutation, either fixed or in heterozygosis, showed a yellow to orange color. In the cluster for each genotype, we observe a separation from the transgenic lines to their relatives without transgene (Figure 4C). The fruits from these plants also showed a yellow coloration in their inner part; the color change in the placenta is the most obvious. Plants without mutant alleles from B^{Sh} showed a yellow color similar to TF, and plants with the B^{Sh} fixed showed a more intense yellow color (Figure 4D).

We analyzed saffron apocarotenoid accumulation in the fruits of the F2 and F3 populations (Figure 5). In both populations, the plants harboring the fixed B^{Sh} mutation showed a significantly higher accumulation of crocins than non-mutant plants. The mutation affected crocin accumulation even in heterozygosis, as can be seen in F2 68, F3 68B, and the F1 plants, whose fruits accumulated an intermediate amount of crocins between those of fruits from the non-mutant and the homozygous mutant plants. However, none of the F2 plants produced fruits accumulating levels as high as Xantoffron 1A. Interestingly, the two plants from the F3 population that harbored all Xantomato mutations (F3 26B and 66A) accumulated fewer crocins than their siblings with less fixed mutations, having similar levels to those with B^{Sh} mutation in heterozygosis (Figure 5A,B). A similar trend was observed with HTCC accumulation in both populations. Plants harboring the B^{Sh} mutation accumulated higher levels of HTCC. Plants with the B^{Sh} alleles from MM but harboring *hp3* and/or $hp2^{dg}$ mutations accumulated more HTCC in the fruits than those without *hp* mutations (Figure 5C,D).

Plants with the *hp3* mutation accumulated higher levels of picrocrocin. Contrary to what happens with crocins and B^{Sh}, the data suggest that other factors influence picrocrocin accumulation, probably the presence of $hp2^{dg}$ mutation either in heterozygosis or homozygosis (Figure 5E,F).

Engineering *Cs*CCD2 levels in tomato fruits of diverse carotenoid mutant combinations affect carotenoids

These materials are ideally suited to elucidate which are the preferred substrates of *Cs*CCD2 in tomato and to see if there is an effect on carotenoid metabolism in tomato fruit due to the expression of the transgene or to the accumulation of saffron apocarotenoids. We evaluated the carotenoid accumulation in the F1, F2, and F3 fruit resulting from the cross of Xantomato with TF.

Fruits that expressed *CsCCD2* in genetic backgrounds that typically accumulate lutein and/or zeaxanthin failed to accumulate lutein nor zeaxanthin, confirming that these two carotenoids are the preferred substrate for the cleavage by *Cs*CCD2. Plants harboring the B^{Sh} mutation either in homo or hemizygous state accumulated β-carotene as their primary carotenoid in the fruit. In contrast, fruits from non-mutant plants had lycopene as the primary carotenoid. This carotenoid profile is due to the higher expression levels of *CYCB* and, in some cases, of *LCYb1* in the fruits from mutant plants. The plants containing the saffron cassette and the B^{Sh} mutation showed a lower expression of *BCH1* and *BCH2* than Xantomato (Figure 6).

All plants homozygous for $hp2^{dg}$ (except F2 66) accumulated significantly higher amounts of total carotenoids in the fruit than the other plants and showed higher expression levels of MEP and carotenoid pathway genes. The primary carotenoid in these fruits is determined by the genotype of B^{Sh} (Figure 6). Interestingly, Xantomato accumulated low levels of phytoene, while F2 and F3 plants harboring any *hp* mutation fixed (except F2 35) accumulated significantly higher levels of this early carotenoid (Figure S4A,B).

All F3 plants with the B^{Sh} mutation fixed showed β--cryptoxanthin accumulation. Almost all F3 plants accumulated γ-carotene and/or α-carotene (Figure S5). Some plants increased significantly the β-carotene content in the fruit compared to Xantomato. In the F2 generation, these were all plants with the B^{Sh} mutation fixed; however, in the F3 generation, this increase was only observed in the plants containing at least one mutated allele of $hp2^{dg}$ (Figure S4E,F).

A subchromoplast fractionation was performed in plants with B^{Sh} mutation fixed to determine if there is any change in the carotenoid subplastidial location. MM and TF showed two sectors of high carotenoid accumulation, comprised between fractions 18 and 28, consisting of membranes. In contrast, F3 90A exhibited four accumulation sections from fraction 22 to fraction 34 (Figure S6), indicating that in F3 90A fruits, carotenoids are accumulated in the submembrane compartments and the stroma. We did not detect crocins or picrocrocin from fraction 23 to fraction 27 in TF and F3 90A (data not shown). Crocins and picrocrocin were detected in the supernatant from the first centrifugation before the chromoplast fractionation in TF and F3 90A but not MM. These results confirm that the chromoplast is not the main storage compartment for crocins and picrocrocin.

Changes in tomato plant yield and quality by the introduction of the saffron cassette and carotenoid mutations

In the F3 population, a positive correlation between $hp2^{dg}$ and *hp3* mutations with a high percentage of BER and higher fruit firmness was observed, together with a strong negative correlation with number of seeds, fruit weight, and the diameter of the fruits. The $hp2^{dg}$ mutation exhibited the strongest negative effect on tomato yield (Figure S7). Fortunately, we did not observe a negative correlation between these traits and B^{Sh} mutation, which had the most substantial effect on crocin and HTCC accumulation. The *hp* mutations were correlated to overexpression of carotenoid and MEP pathway genes, except for *BCH1*, which we have observed is down-regulated when there is *CsCCD2* expression (Figure 7B).

The most critical mutation for clustering based on saffron apocarotenoid accumulation is B^{Sh} (Figure 7A). The total yield of crocins and picrocrocin was calculated based on the number of fruits per plant, the fruit weight (Figure S7), and the normalized values of both saffron apocarotenoids (Figure 7C). The plant with the highest

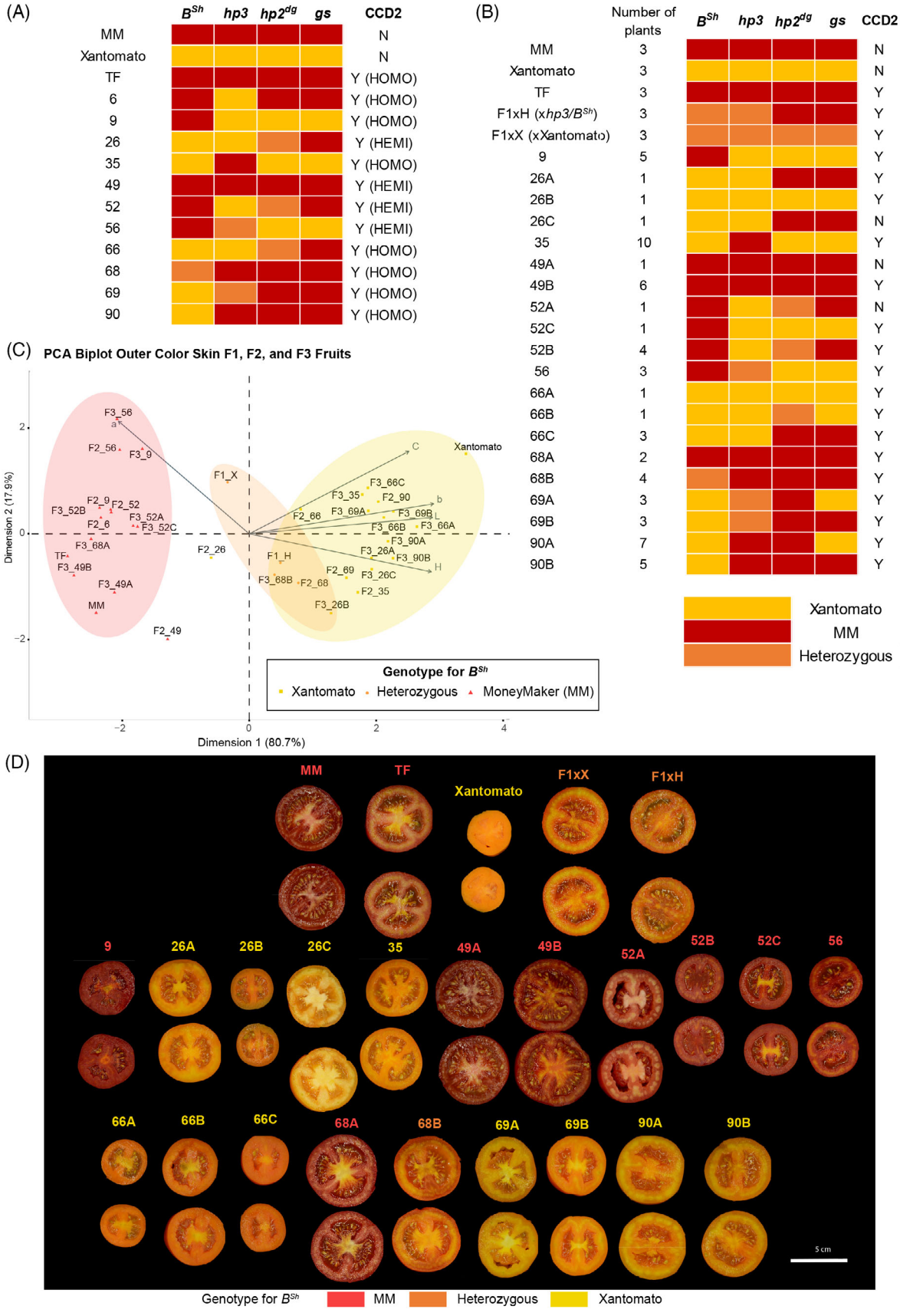

Figure 4. Genotyping results of the F2 (A) and F3 (B) plants generated from the cross of TF and Xantomato. *Cs*CCD2 presence (Y) or absence (N). HOMO: homozygosis of the transgene, HEMI: hemizygosis of the transgene. (C) Principal component analysis (PCA) biplot with the skin color parameters (C, L, a, b, H). The percentage of variance explained by the first and second components is indicated in the axes. Each symbol represents the mean of three fruits per plant (n = 3). Symbols are colored based on the plants' B^{Sh} genotype. The variable arrows represent the contribution of each variable on each component. (D) Phenotype of the inner part of parentals, F1, and F3 fruits, coloring based on the B^{Sh} genotype.

levels of crocins and picrocrocin per square meter was 26A, accumulating 6 and 14.7 times more crocins and picrocrocin than TF. F3 66B accumulated higher levels of picrocrocin but half the amount of crocins; in addition, F3 66 plants produced very few seeds, while F3 26A plant produced plenty of seeds. The following best plants are F3 69 and F3 90, which accumulate high levels of crocins but not as high levels of picrocrocin. The presence of B^{Sh} resulted in high levels of crocins, and in combination with *hp3*, there was a high accumulation of both crocins and picrocrocin (Figure 7C).

DISCUSSION

The combination of B^{Sh} and *hp3* mutations and the saffron cassette results in the highest yields of saffron apocarotenoids obtained in heterologous viable platforms

Up to now, tomato fruit has been the platform where the highest levels of crocins were obtained. The initial TF accumulated up to 14.5 mg/g of crocins and 3 mg/g of picrocrocin in tomato fruit DW (Ahrazem, Diretto, et al., 2022). Crocin levels were increased 1.5-fold in tomato fruit DW by crossing TF with *hp3*/B^{Sh}. However, the ratio of crocin accumulation compared to TF could be lower due to the weight loss caused by the *hp3* mutation (Morote, Lobato-Gómez, et al., 2023). Similar results were obtained in *N. benthamiana*, where the infiltration of edited plants accumulating high levels of zeaxanthin in the leaves resulted in higher crocin levels (Demurtas et al., 2023).

Combining the four Xantomato mutations and the saffron cassette was initially our most promising approach to boosting saffron apocarotenoid accumulation in tomato fruit, and indeed, we obtained very high levels of crocin accumulation in the Xantoffron 1A line (Figure 2). Unfortunately, the plants from this line showed highly deleterious effects on plant growth and fruit development. The high levels of saffron apocarotenoid accumulation in the fruits are rather unlikely to have caused this phenotype; the biosynthesis of these compounds was targeted in the fruit after ripening using the E8 fruit-specific promoter, and Xantoffron 9 showed similar negative plant growth effects and accumulated significantly lower levels of crocins (Figure 2). Interestingly, we have found similar results in our approach to dissecting Xantomato mutations. In the F3 generation, two plants with the four Xantomato mutations and the saffron cassette, obtained from two independent F2 plants, showed deleterious effects on plant growth and fruit weight (Figure S7) and resulted in a low yield of crocins production (Figure 7C). Taken together, these results demonstrate that this combination is not practical for producing high amounts of saffron apocarotenoids on a large scale. Our results in the F2 and F3 generations from the cross of TF with Xantomato indicated evidence that the $hp2^{dg}$ mutation is the one having the most detrimental effect on plant growth, as the presence of this mutation in homozygosis is negatively correlated with fruit weight, number of fruits per plant, and number of seeds per fruit (Figure 7B; Figure S7). In addition, our results suggest that the adverse effects on plant growth and development occur when this mutation is combined with the other *high-pigmented* mutation, *hp3*, as the best-performing plant with the $hp2^{dg}$ mutation fixed in terms of saffron apocarotenoids yield does not contain the *hp3* mutation (Figure 7C; Figure S7).

Interestingly, we found that B^{Sh} mutation is sufficient to obtain high levels of crocins in tomato fruit of our engineered plants (up to 12-fold and 8-fold increase by DW in the F2 and F3 generations compared to TF), showing that the boost of the carotenoid biosynthetic pathway towards β-carotene accumulation is sufficient to accumulate high levels of crocins, as previously observed (Morote, Lobato-Gómez, et al., 2023). The B^{Sh} mutation has been demonstrated to be semi-dominant for β-carotene accumulation (Ronen et al., 2000), and we have observed similar results for crocin accumulation; F2 and F3 plants were clearly classified in terms of crocin accumulation: high (homozygous mutation), intermediate (heterozygous mutation), low (non-mutants) crocin levels (Figure 5A,B). This is a very interesting result, as β-carotene is not used as a substrate for *Cs*CCD2 (Frusciante et al., 2014). We did not observe overexpression of *BCH1* or *BCH2* in plants carrying the B^{Sh} mutation (Figure 6C), suggesting that the increase of its substrate is enough for tomato BCHs expressed at basal levels to convert β-carotene to zeaxanthin, which will be subsequently cleaved by *Cs*CCD2 to produce crocins. Neither an increase of *CYCb* nor *LCYb1* expression was observed in B^{Sh} transgenic and mutant plants compared to the non-transgenic B^{Sh} mutant plants (Figure 6C), showing that the accumulation of crocins or the *CsCCD2* expression do not activate these genes at the transcriptional level. During the process of obtaining Xantomato, it was determined that B^{Sh} mutants and *hp3*/B^{Sh} mutants accumulated 5 and 7 times less zeaxanthin than Xantomato but 50 and 75 times more zeaxanthin than M82

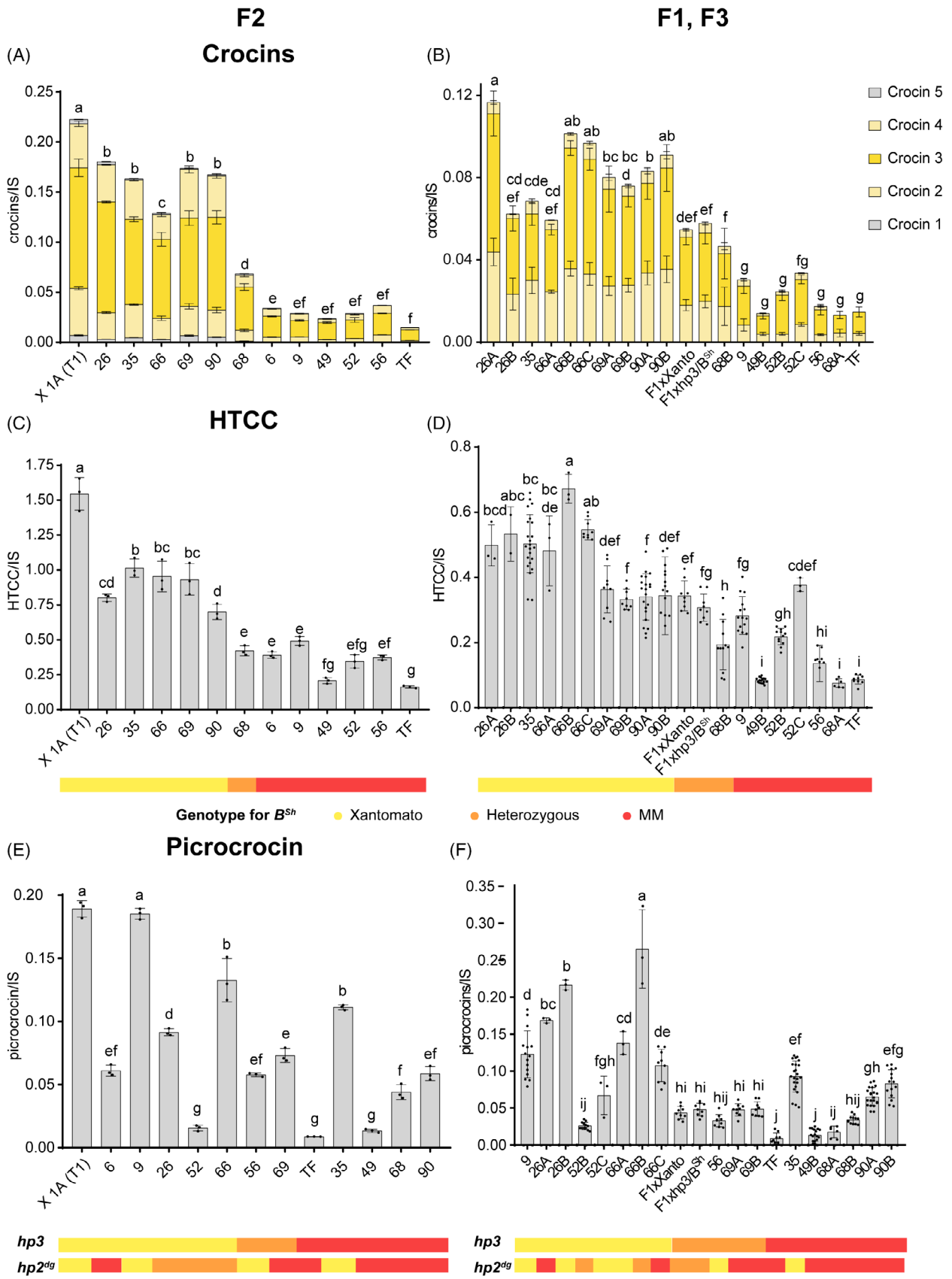

Figure 5. Results of F1, F2, and F3 fruits from the cross of Xantomato with TF. (A, B) Relative crocin accumulation, quantified via LC–MS and normalized with genistein as internal standard (IS). (C, D) Relative HTCC accumulation, quantified via LC–MS and normalized with genistein as IS. (E, F): Relative picrocrocin accumulation, quantified via LC–MS and normalized with genistein as IS. Line grouping is based on an ANOVA test for total metabolite content in each graph, followed by a Tukey post-hoc test. Plants are organized based on the genotyping results from the mutation that showed a higher discrimination on each variable on the PLS-DA (Figure S2). Error bars represent the SD of biological replicates ($n \geq 3$).

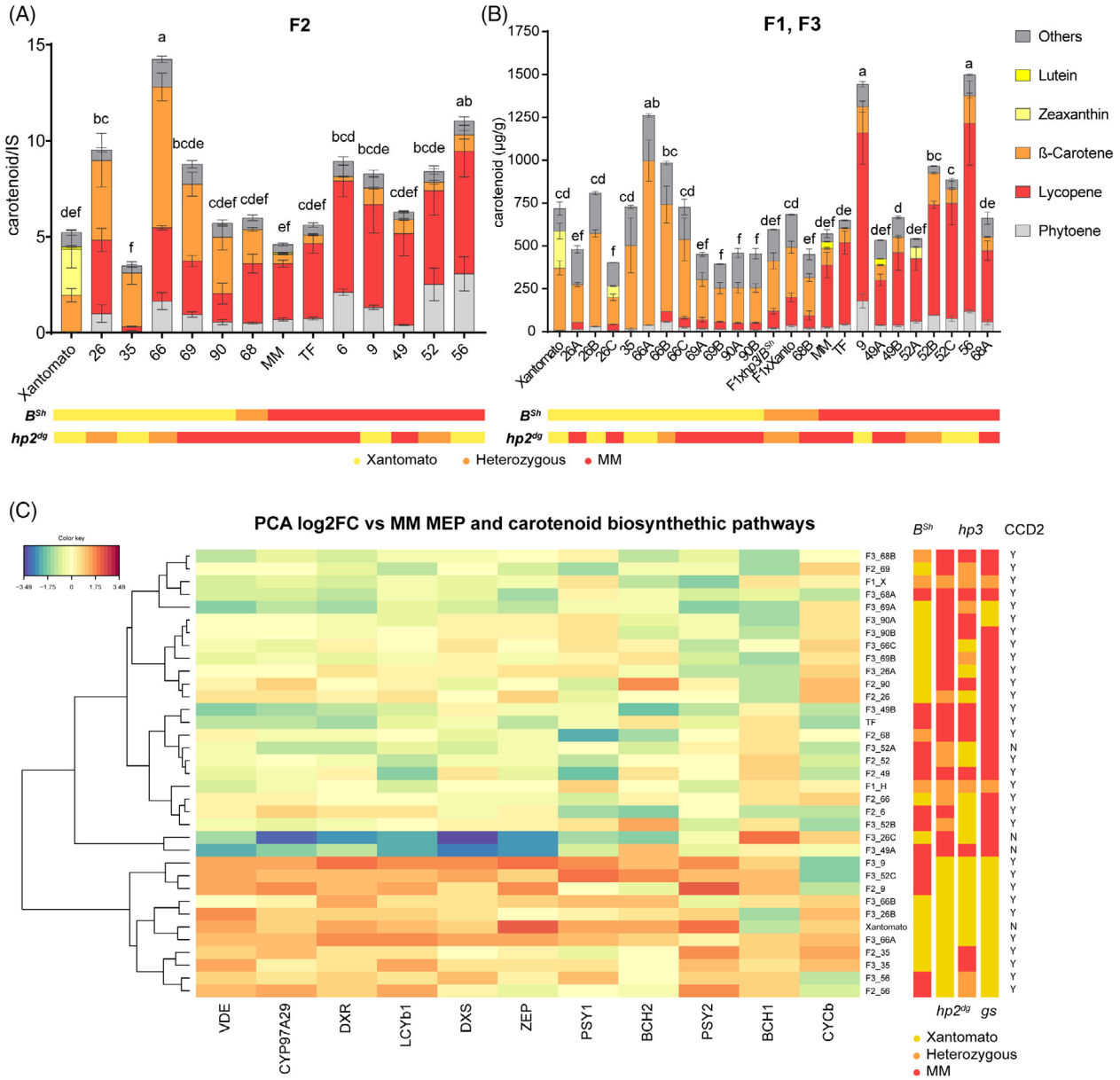

Figure 6. Carotenoid contents in F1, F2, and F3 fruits from the cross of Xantomato with TF. (A) Relative carotenoid accumulation on the F2 population, quantified via HPLC-PDA and normalized with canthaxanthin as internal standard. (B) Absolute carotenoid accumulation on the F1 and F3 population, quantified via UPLC-PDA and using standard curves. Line grouping is based on an ANOVA test for total metabolite content in each graph, followed by a Tukey post-hoc test. Plants are organized based on the genotyping results from the mutation that showed a higher discrimination on each variable on the PLS-DA (Figure S2). Error bars represent the SD of biological replicates ($n = 3$). (C) Clustered Image Map from the Principal component analysis (PCA) applied to the qPCR results of MEP pathway and carotenoid biosynthesis genes. The x-axis shows the gene variables. The y-axis shows the genotype, colored according to their genotype in the Xantomato mutations. The qPCR data used to perform the PCA is the log2FC of the $2^{-\Delta\Delta Ct}$ using wild-type MoneyMaker as control. The values of each genotype are the mean of biological replicates ($n \geq 3$).

The Plant Journal, (2024), doi: 10.1111/tpj.17030

(A)

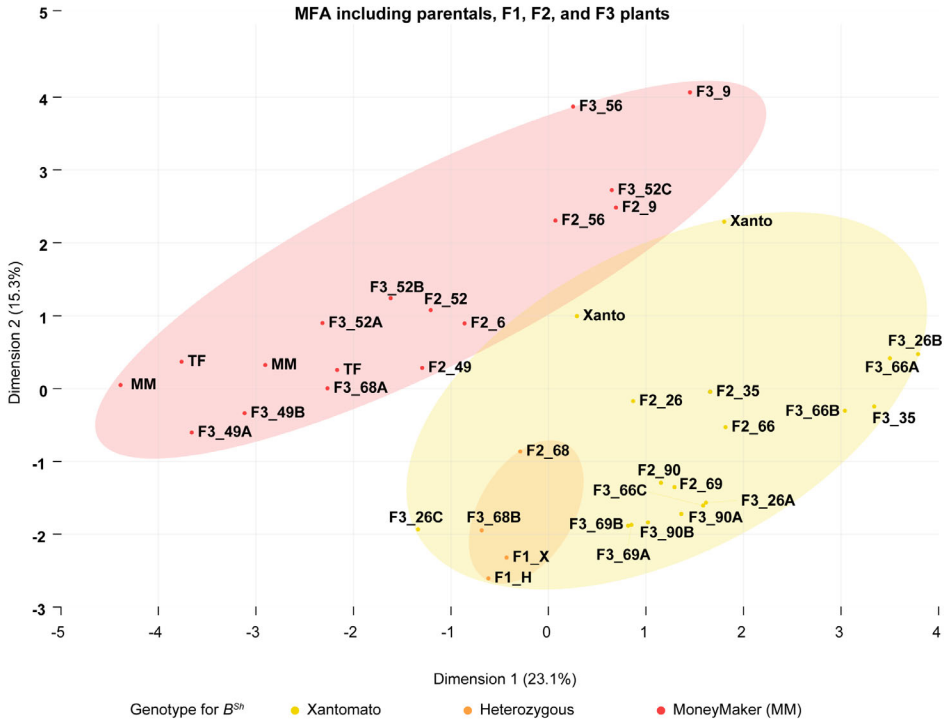

(B)

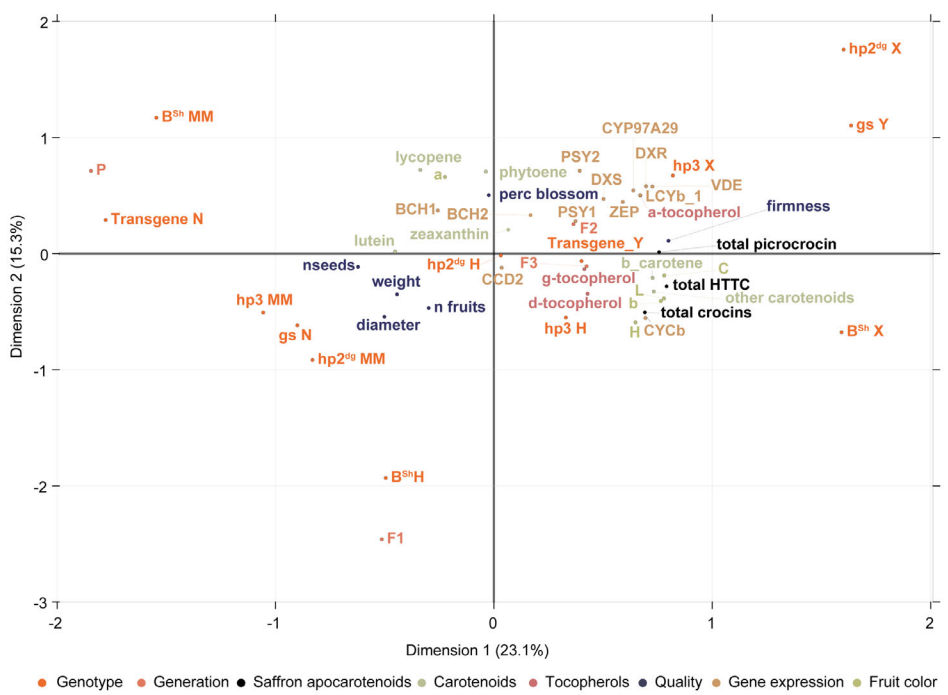

(C) **Saffron apocarotenoid and carotenoid yield per plant compared to TF**

	26A	66C	69B	69A	90A	F1xX	90B	66B	F1xH	68B	35	66A	52B	49B	52C	68A	TF	26B	9	56
Crocins (C)	6.1	5.6	4.3	4.3	3.9	3.9	3.7	3.6	3.3	2.7	2.5	2.1	1.3	1.1	1.1	1.0	1.0	1.0	0.5	0.2
Picrocrocin (P)	14.7	10.5	4.6	4.3	5.1	4.9	5.6	15.9	4.8	3.3	5.6	8.1	2.3	1.6	3.6	2.2	1.0	5.6	3.1	0.5
Ratio P/C	2.4	1.9	1.1	1.0	1.3	1.3	1.5	4.4	1.5	1.2	2.3	3.9	1.8	1.5	3.3	2.2	1.0	5.8	6.8	3.1
Total carotenoids	0.6	1.0	0.5	0.6	0.5	1.0	0.4	0.8	0.8	1.2	0.6	1.0	1.2	1.2	0.7	1.2	1.0	0.3	0.5	0.3
B^{Sh}																				
hp3																				
hp2^{dg}																				
gs																				

Figure 7. Multiple Factor Analysis (MFA) of qualitative (genotype, generation) and quantitative (saffron apocarotenoids, carotenoids, tocopherols, quality, gene expression, fruit color) variables analyzed in the parental, F1, F2, and F3 plants from the TF x Xantomato cross. The percentage of variance explained by the first and second dimensions is indicated in the axes. (A) Graph of individuals, colored by genotype in B^{Sh}. Each symbol represents the mean of the biological replicates per genotype ($n \geq 3$). The two points of each parental or control line (Xantomato, TF, and MM) represent their values in each generation (F2 and F3). (B) Graph of variables, colored by groups, showing the relationship between variables and their correlation with the dimensions. (C) The ratio of crocin, picrocrocin, and carotenoid yield in F1 and F3 plants using TF as the reference line. The yield of crocin and picrocrocin was calculated by multiplying the mean of the number of fruits per plant, the median of the fruit weight per plant (Figure S7), and the normalized values of crocin, picrocrocin (Figure 5B,F), and total carotenoids (Figure 6B).

(Karniel et al., 2020). In our F1, F2, and F3 plants with the saffron cassette, all zeaxanthin is cleaved by *Cs*CCD2 as we cannot detect it (Figure 6A,B), suggesting that the higher levels of crocins in the B^{Sh} mutants are due to the significantly higher levels of zeaxanthin available in the mutant fruits compared to non-mutant ones. In addition, the F2 and F3 plants carrying B^{Sh} alone or B^{Sh} together with other Xantomato mutations accumulate similar amounts of crocins in the fruit (Figure 5A,B), suggesting that there is an increase in the zeaxanthin flux when *Cs*CCD2 is consuming it, and this flux compensates the lower initial levels of zeaxanthin in the single mutants for B^{Sh} compared to the double, triple, or quadruple mutants.

In all the plants analyzed in this study, the major crocin was crocin 3, followed by crocin 2 or crocin 4 (Figures 2, 3 and 5), which is consistent with previous studies where crocins have been produced in tomato fruit (Ahrazem, Diretto, et al., 2022; Frusciante et al., 2022; Morote, Lobato-Gómez, et al., 2023). In *C. sativus*, comparable results were observed 2 days after anthesis stigma, where crocin-3 (R1 = beta-D-gentiobiosyl, R2 = beta-D-glucosyl) was the major crocin and its accumulation was correlated with a higher expression of *CsUGT2*, followed by crocin-2 (R1 = R2 = beta-D-glucosyl) and crocin-4 (R1 = R2 = Beta-D-gentiobiosyl) (Moraga et al., 2009). *CsUGT2* is expressed constitutively in tomato fruit, thus explaining why the major crocin is always crocin-3. Interestingly, *hp* mutations, especially *hp3*, boosted the accumulation of picrocrocin (up to 21-fold to 30-fold increase in DW in the F2 and F3 generations compared to TF).

The fruit weight and the number of fruits per plant should be considered to factor in the effect of the carotenoid mutations on the total saffron apocarotenoid yield. The DW accumulation of crocin and picrocrocin in all F3 plants has been calculated and compared to TF (Figure 7C). Among the top 5 plants that accumulated similar levels of crocins, the accumulation of picrocrocin is up to 3 times higher in the plants harboring the *hp3* mutation compared to the ones that do not. These differences in crocin and picrocrocin accumulation based on the *hp3* genotype could be due to higher levels of zeaxanthin converted to saffron apocarotenoids in these mutants caused by the block of its conversion to violaxanthin/neoxanthin (Galpaz et al., 2008). However, this does not explain why the levels of HTCC do not correlate with the ones of picrocrocin. Another hypothesis is related to the different transport and storage of these apocarotenoids. While it has been demonstrated that crocins are transported to the vacuole by ABCC transporters in *C. sativus*, the transporters for picrocrocin have not been identified (Demurtas et al., 2019). The accumulation of crocins in tomato fruit without engineering these ABCC transports suggests that crocins are transported to the vacuole by endogenous ABCC transporters. We have observed that picrocrocin is not stored in the chromoplast (data not shown), which was expected due to its hydrophilic glycosylated nature. Nevertheless, the transport of picrocrocin to the vacuole could be mediated by a different transporter from those of crocins, and it could be that the *hp3* mutation positively affects that.

F3 26B and 66A contained all Xantomato mutations but accumulated similar levels to that of the heterozygous plants. The lower accumulation levels, observed also in F3 35, could be due to an adverse effect of the $hp2^{dg}$ mutation on crocin levels. However, F2 35 has the same genotype as F3 35 and did not show this behavior (Figure 5A–D). In the F3 generation, we could detect the negative effect on plant yield and, consequently, on crocin accumulation of the $hp2^{dg}$ mutation, but in the F2, we could not. This negative effect of $hp2^{dg}$ in the F3 population is reflected in Figure 6C, where none of the plants harboring this mutation are among the ones with the highest yields of crocin and picrocrocin accumulation. On the other hand, *gs* mutation did not seem to affect saffron apocarotenoids accumulation because no differences were observed between F3 69A and 90A (*gs* mutants) and F3 69B and 90B (*gs* non-mutants) plants (Figure 7C).

Our results demonstrated that B^{Sh} and *hp3* mutations are the most relevant mutations in terms of saffron apocarotenoid accumulation. It is important to consider that TF is coming from a MM background. In contrast, Xantomato is obtained from the cross of different genetic backgrounds containing the mutations of interest, including a M82 mutant (*hp3* mutation) (Galpaz et al., 2008), a mutant from cv. Manapal ($hp2^{dg}$ mutation) (Bino et al., 2005), a 'Jaune Flamme' hairloom tomato line (B^{Sh} mutation), and the tomato line LA0212 (*gs* mutation) (Karniel et al., 2020). The combination of the different genetic backgrounds of both parental lines resulted in several combinations of the four mutations of interest, but also a high diversity in other genome regions. This indicates that not only the four

mutations we select could influence saffron apocarotenoid accumulation and yield, but also other regions linked to these mutations that we are not considering. In the F3 siblings where a considerable number of plants were obtained, such as F3 35, 69A, 69B, 90A, and 90B, plants produced fruits with different shapes (data not shown), and in the case of F3 35, F3 90A, and 90B, a high dispersion of fruit weight depending on the plant was observed (Figure S7); however, the metabolite results did not show a high variability between plants (Figure 5B,D,F, Figure 6B), and neither a high variability between genotypes (all of them containing the B^{Sh} mutation), thus demonstrating that Xantomato mutations are the genomic regions having the primary effect on the accumulation of saffron apocarotenoids and carotenoids in tomato fruit. The variability in other traits, including fruit shape and weight, will help us select the best siblings in each generation while obtaining fixed lines.

The expression of *CsCCD2* with Xantomato mutations results in a diversification of carotenoids

In our engineered tomatoes, B^{Sh} was the mutation that determined the primary carotenoid of the fruits. The mutation resulted in the accumulation of mainly β-carotene instead of lycopene, but as previously demonstrated, it did not result in a higher accumulation of total carotenoids (Ronen et al., 2000). In contrast, the *high pigmented* mutations were responsible for the higher level of carotenoids in our transgenic plants, as has been observed previously by the increase of 30% in the total carotenoids in *hp3* tomato (Galpaz et al., 2008) and by the 2.5-fold increase in lycopene accumulation in $hp2^{dg}$ mutants compared to the non-mutant plants (Levin et al., 2003). The semi-dominant effect of B^{Sh} was already observed in F1 plants resulting from the TF x $hp3/B^{Sh}$ and TF x Xantomato crosses (Figure 3). The other three mutations are recessive (Galpaz et al., 2008; Karniel et al., 2020; Levin et al., 2003) and should not affect carotenoid and saffron apocarotenoid accumulation. Nevertheless, the fruits from the cross with Xantomato produced higher levels of carotenoids and saffron apocarotenoids. This could be because other genomic regions differ between Xantomato and $hp3/B^{Sh}$ parental lines, affecting carotenoid accumulation.

In the F3 population, only the plants with the B^{Sh} mutation and the $hp2^{dg}$ mutation either in homozygosis or heterozygosis showed a significantly higher accumulation of β-carotene than Xantomato (Figure S4F), as observed with the Xantoffron lines (Figure 2E). When the B^{Sh} mutation was absent, lycopene accumulation was significantly higher than in MM when the *hp2dg* mutation was present (Figure S4D). These results suggest the engineered apocarotenoids possible forward feed role on the fruit endogenous carotenoid pathway that led to new carotenoid/apocarotenoid fortification in the $hp2^{dg}$ context. The combination of B^{Sh} and $hp2^{dg}$ resulted in very high levels of β-carotene and saffron apocarotenoids. However, the $hp2^{dg}$ mutation negatively affects plant growth and yield (Figure 7B). The $hp2^{dg}$ phenotype results from the mutation of the tomato homolog for *Arabidopsis thaliana* DE-ETIOLATED1 (DET1) (Mustilli et al., 1999), but has collateral effects on plant growth and yield (Rao Davuluri et al., 2005). RNAi-mediated suppression of DET1 in the fruit resulted in plants with the desired phenotype but no deleterious effects on plant growth (Rao Davuluri et al., 2005), suggesting that the negative effect of the $hp2^{dg}$ mutants on the plant yield of our F3 plants are not caused by close genomic regions linked to the $hp2^{dg}$ mutation but by the mutation. The combination of $hp2^{dg}$ and the saffron cassette could be improved by the specific silencing of DET1 in the fruit in the best fixed lines with the saffron cassette and B^{Sh} and *hp3* mutations.

In previous studies, it has been observed a regulatory feedback mechanism of apocarotenoids in carotenoid biosynthesis: in *Arabidopsis thaliana*, the exogenous application of β-cyclocitral, an apocarotenoid derived from the cleavage of β-carotene, down-regulated the MEP pathway (Mitra et al., 2021). In tomato, the epistatic effect of *tangerine* mutation over the *yellow-flesh* mutation could be due to the signaling effect of a *cis*-configured apocarotenoid derived by CCD cleavage of neurosporene or prolycopene (Kachanovsky et al., 2012) and a zeaxanthin or antheraxanthin apocarotenoid showed a negative feedback regulation on carotenoid biosynthesis in transgenic lines with high expression of β-cyclase and β-hydroxylase in tomato ripe fruits (D'Ambrosio et al., 2023). In contrast, our results suggest regulatory positive feedback operating upstream and throughout the carotenoid pathway when the $hp2^{dg}$ mutation was present due to the increase in the expression of almost all MEP and carotenoid biosynthetic pathway genes (Figure 6C). This significant increase in carotenoid content was not observed in the absence of $hp2^{dg}$. Instead, the plants accumulated similar or lower amounts of total carotenoids compared to their parental lines (Figure 6B), indicating that the levels of the xanthophyll-derived apocarotenoid that causes a negative feedback regulation on the carotenoid biosynthesis (D'Ambrosio et al., 2023) must be produced at lower levels in our transgenic lines because zeaxanthin is cleaved by *Cs*CCD2 to produce saffron apocarotenoids.

Overall, plants accumulating saffron apocarotenoids with different carotenoid profiles were obtained. The F1 fruits from both Xantomato and $hp3/B^{Sh}$ crosses accumulated considerably higher levels of both crocins and picrocrocin than the original TF line and high levels of β-carotene and lycopene (Figure 3). These plants are good candidates for being a source of antioxidant metabolites in tomato fruit's liposoluble and hydrophilic fractions. In contrast to what happened in TF (Ahrazem, Diretto, et al., 2022), we did not observe an overall reduction in

total carotenoid accumulation but maintenance of the levels or a significant increase when the *hp2*^{dg} mutation was present. However, the carotenoid yield per plant was affected compared to TF in the *hp2*^{dg} mutants due to the production of smaller and fewer fruits. Different plants with good yield, high levels of crocins and picrocrocins, and a non-affected carotenoid accumulation were obtained in the present study, including plants with high levels of β-carotene, lycopene, or both (Figures 6 and 7C).

In this study, the skin color of the fruit was determined by the carotenoid profile and not the saffron apocarotenoid accumulation (Figure 4C). This seems to be a characteristic observed when the CCD that produces saffron apocarotenoids is expressed under the control of a fruit-specific promoter (Ahrazem, Diretto, et al., 2022; Morote, Lobato-Gómez, et al., 2023) but not when it is expressed with the 35S promoter, as observed with the transformation of *S. lycopersicum* cv. MM with *Cs*CCD2 (Ahrazem, Diretto, et al., 2022) and of *S. lycopersicum* cv. MicroTom with *Bo*CCD4-3 (Frusciante et al., 2022), where the fruits showed an orange outer color of the fruit, compared to the red color of the wild-type, corresponding to a reduction of total carotenoid accumulation (Ahrazem, Diretto, et al., 2022).

High levels of saffron apocarotenoid accumulation require minimal *CsCCD2* expression and lead to depletion of lutein and zeaxanthin substrates

Our results showed a correlation between both saffron apocarotenoids accumulation/zeaxanthin and lutein consumption and *Cs*CCD2 mRNA levels in the fruit of Xantoffron lines (Figure 2B,C,D); this did not occur in the fruit of the F2 plants from the TF x Xantomato cross, where both carotenoids were consumed by *Cs*CCD2 independently of the *Cs*CCD2 mRNA levels. The saffron apocarotenoid accumulation was not influenced by the hemizygosis or homozygosis of the transgene but by the genotype for the Xantomato mutations (Figures 5 and 6; Figure S3; Table S5). In a *N. benthamiana* experiment, it has been observed that the infiltration of *Cs*CCD2 driven by the 35S promoter did not result in all zeaxanthin consumption. In contrast, the overexpression of *Cs*CCD2 with a TEV vector resulted in zeaxanthin depletion in the leaves (Demurtas et al., 2023). These results suggest that a minimum expression of *Cs*CCD2 is required for the enzyme not to be limiting. Once this is achieved, the limiting factor for saffron apocarotenoid accumulation is not the *Cs*CCD2 expression but most likely substrate availability.

Xantoffron 9 line showed a lower accumulation of crocins than TF but similar levels of HTCC and picrocrocin value (Figure 2C,D). From one molecule of lutein or zeaxanthin, one or two molecules of picrocrocin are obtained, respectively. This can explain why there is a higher accumulation of picrocrocin but lower levels of crocins in Xantoffron 9 compared to TF. The carotenoid profile of Xantoffron 9 suggests that *Cs*CCD2 uses zeaxanthin as its preferred substrate to produce saffron apocarotenoids when the expression of the gene is low and that both carotenoids are consumed when the expression levels achieve a minimal threshold value (Figure 2B,E). Consistent with that, in a previous *in vitro* assay it was observed that the conversion rate of zeaxanthin by *Cs*CCD2 was higher than that of lutein (Frusciante et al., 2014).

Lutein and zeaxanthin are the only carotenoid substrates used by *Cs*CCD2

It has been demonstrated *in vitro* that *Cs*CCD2 can cleave zeaxanthin, lutein, and 3-OH-β-apo-8′-carotenal but does not cleave β-carotene, violaxanthin or β-cryptoxanthin (Frusciante et al., 2014). In the fruits of all TF transgenic lines, lutein was the only carotenoid completely converted, indicating that this was the preferred substrate used by *Cs*CCD2. It was observed that phytoene, phytofluene, α-carotene, β-carotene, and lycopene levels were lower in transgenic lines, but these carotenoids did not disappear (Ahrazem, Diretto, *et al.*, 2022). Similar results were observed in tomato plants with high levels of β-carotene in the fruit expressing *CsCCD2*; β-carotene levels were lower than in the non-transgenic plants (Morote, Lobato-Gómez, et al., 2023). These results are similar to those obtained with *Sh*CCD4b overexpression in *S. lycopersicum*, where β-carotene and lutein were converted by ShCCD4b and not detected in the fruit, and lycopene was not converted; however, its levels were reduced (Yoo et al., 2023). The decrease in the carotenoids that are not used as a substrate for the CCDs appears to result from a feedback regulation rather than partial conversion by the CCD. This did not occur with the plants fixed for the *hp2*^{dg} mutation. All these plants showed an apparent up-regulation of the MEP and the carotenoid biosynthetic pathway (Figure 6C). In addition, transgenic plants with the *hp2*^{dg} mutation showed a significantly higher accumulation of phytoene compared to Xantomato (Figure S4A,B) and a significantly higher accumulation of lycopene in the case of plants with no *B*^{Sh} alleles and of β-carotene in the case of plants with *B*^{Sh} alleles (Figure S4C–F). This increase in carotenoid content did not result in higher levels of crocin accumulation (Figure 5A,B), strongly supporting that these three carotenoids are not substrates for *Cs*CCD2 *in vivo* because their levels were increased in the presence of the enzyme, and the crocin levels were not affected.

Non-transgenic Xantomato and F3 26C, a plant with *hp3* and *B*^{Sh} mutations and no transgene, accumulated β--cryptoxanthin, γ-carotene, and α-carotene, and plants harboring the same combination of mutations with the transgene also accumulated these carotenoids at similar levels (Figure S5), leading to the conclusion that *Cs*CCD2 does not use them as substrates *in vivo*, as previously demonstrated *in vitro* (Frusciante et al., 2014).

In this work, we have demonstrated *in vivo* that lutein and zeaxanthin are most likely the only carotenoids used as substrates for *Cs*CCD2 in tomato fruit, and that the highest levels of crocin and picrocrocin accumulation are achieved in transgenic Xantomato plants. However, these plants do not show robust plant growth and fruit development characteristics. Therefore, the four mutations present in the Xantomato have been dissected to elucidate the best combination for obtaining high levels of crocins and picrocrocin in plants without compromising plant growth and fruit production. The results have demonstrated that the presence of the B^{Sh} mutation alone increases the crocin accumulation significantly and that the presence of the *hp3* mutation results in increased levels of picrocrocin. The $hp2^{dg}$ mutation, in combination with *CsCCD2* expression, resulted in higher levels of carotenoids in the fruit. Still, the detrimental effects on plant growth and fruit yield are more likely due to the presence of this mutation. Taken together, the best combination of mutations to obtain high levels of saffron apocarotenoids is B^{Sh} and *hp3*, and fixed lines with these mutations selected based on their yield would be a suitable platform to silence *DET1* in the fruit and produce plants with high yields of both saffron apocarotenoids and carotenoids. We have shown that it is possible to select combinations of carotenoid mutations that result in the accumulation of both exotic saffron apocarotenoids and endogenous carotenoids, thus providing high antioxidant levels at both hydrophilic and liposoluble fractions of tomato fruit.

EXPERIMENTAL PROCEDURES

Plant material

S. lycopersicum cv. MM, Tomaffron (Ahrazem, Diretto, et al., 2022), Xantomato, and $hp3/B^{Sh}$ (Karniel et al., 2020) were used as starting material. Tomaffron (TF) was selected as the best-performing fixed line from (Ahrazem, Diretto, et al., 2022) that produced a good yield of fruit and seeds. Tomato plants were grown under greenhouse conditions either at IBMCP in Valencia (2808 h of sun /year, 36.7202° N 4.4203° O) or IHSM La Mayora in Málaga (3248 h of sun/year, 39.4698° N 0.3774° O).

Fully-ripen tomato fruits for analysis were harvested at breaker+10 days (Br + 10) stage at IBMCP or the equivalent Br + 7 at La Mayora, where ripening occurred faster (as assessed by Hunter lab colorimeter). Sectors of the pericarp of the tomatoes were collected, snap-frozen in N_2 (l), and stored at −80°C. For each plant, a pool of pericarp samples from three to five tomatoes was freeze-dried and stored at −80°C until further analyses.

Agrobacterium-mediated transformation of Xantomato

The saffron cassette (O1 construct from (Ahrazem, Diretto, et al., 2022)) was used to transform Xantomato. This cassette contained *CsCCD2* under the control of E8 fruit-specific promoter and *CsUGT2* and *CsUGT709G1* under the control of 35S promoter. *A. tumefaciens* LBA4404 strain carrying the saffron cassette was used to transform cotyledons of Xantomato as previously described (Ellul et al., 2003). Transgenic plantlets (named Xantoffron) were selected on hygromycin and genotyped to confirm the presence of transgenes. Primers used to genotype the transgenes are listed in Table S1. All Xantoffron plants were grown in the IBMCP greenhouse.

TF x Xantomato and related crosses

TF, $hp3/B^{Sh}$, and Xantomato plants were grown in the IBMCP greenhouse and used for the intended crosses. A subset of flowers was emasculated one day before anthesis and manually pollinated with pollen from the donor plant collected from flowers at anthesis on the same day. F1 plants were grown at the IBMCP to characterize their phenotype and to obtain F2 seeds. F2 plants carrying the saffron cassette were selected on hygromycin and genotyped for Xantomato mutations, as in (Karniel et al., 2020). Selected F2 plants were grown in the IBMCP greenhouse, and F3 plants were cultivated in IHSM La Mayora greenhouse, with TF, Xantomato, MM, and F1 plants.

Fruit and plant phenotyping

Fruits at the selected ripening stage were harvested and weighed, and their color was measured in three equatorial positions using a Portable Colorimeter CR-400 (Konica Minolta, Tokyo, Japan). F2 and F3 plants were phenotyped for *gs*. For F3 plants, blossom end rot (BER) and the number of fruits per truss were scored. The number of seeds per fruit was counted. Firmness was measured at two equatorial positions using the 53 215 Fruit Hardness Tester (T.R. Turoni, Forlí, Italy).

Sub-chromoplast fractionation

Fruits from MM WT, TF, and F3 90A were used for the sub-chromoplast fractionation. The protocol from (Nogueira et al., 2016) was used. The supernatant containing the cell debris and crocins was stored for further analysis. 34 to 36 sub-chromoplast fractions of 0.9 ml were collected from each gradient. Duplicate sucrose gradients were prepared for each genotype.

Carotenoid and apocarotenoid analyses

Carotenoids were extracted from fruits of Xantoffron, F1, and F2 plants using 10 mg of pericarp powder, spiked with 0.1 μg/ml canthaxanthin as internal standard (IS), and analyzed by HPLC-PDA as previously reported (Barja et al., 2021). Crocins were extracted from 10 mg of powder, spiked with 10 μg/ml genistein as IS, and injected into the LC–MS as previously described (Ahrazem, Diretto, et al., 2022).

Carotenoids and crocins from F3 plants were extracted from 10 mg freeze-dried fruit sample, spiked with 10 μg/mL genistein as IS, or 0.9 ml of each sub-chromoplast fraction, using the protocol on (Perez-Fons et al., 2022). Carotenoids were analyzed by UPLC-PDA, as reported previously (Nogueira et al., 2013), and quantified using standard curves. The polar fraction from sub-chromoplast fractions was freeze-dried, resuspended in 0.8 ml methanol, and centrifuged to discard the precipitated sucrose. All polar fractions were analyzed by UPLC–MS, as previously reported on (Zheng et al., 2021). Feature extraction from chromatogram data files was performed as indicated on (Drapal et al., 2022).

mRNA analyses

RNA was extracted using the NucleoSpin RNA Kit for RNA purification (Macherey-Nagel, Düren, Germany). The RNA was digested with DNAse from the TURBO DNA-free™ Kit (ThermoFisher,

Massachusetts, USA), and subsequently, the cDNA was synthesized using the PrimeScript 1st strand cDNA Synthesis Kit (Takara, Shiga, Japan). The qPCRs were done with the TB Green Premix Ex Taq II (Takara) in a QuantStudio 3 (ThermoFisher). The primers used are listed in Table S2. *S. lycopersicum actin2* was used as the reference gene.

Statistical analyses

All statistical analyses were performed in R. To perform the Principal Component Analysis (PCA) and Partial Least-Squares Discriminant Analysis (PLS-DA) analyses, the Mixomics package was used (Florian et al., 2017), scaling the data. The Multiple Factor Analysis (MFA) was performed using the FactoMineR package (Lê et al., 2008). To use the metabolite results from different data sets in the PLS-DA and MFA analyses, the data from each data set was normalized. The statistical tests used to determine the significant differences between samples or groups or samples were selected according to the distribution of the data, the number of out layers, and the differences of variances between groups.

AUTHOR CONTRIBUTIONS

AG, LGG, PDF, and DO designed the research. MLG, MD, RFM, AE, and SP performed the experiments. MLG analyzed the data and wrote the article. All authors approved the final version.

ACKNOWLEDGMENTS

We thank Prof. Joseph Hirschberg (The Hebrew University of Jerusalem) for providing Xantomato and *hp3/B*^{Sh} seeds. This work was supported by HARNESSTOM (EU H2020 project), contract number 101000716 Innovation Action EC-H2020-SFS-2020-1 and PID2022-141438OB-I00 from the Spanish MCIU. M.L.G. and A.G. are participants of the European COST action CA18210 (ROXY), and this action supported a Short-Term Scientific Mission of M.L.G. at the Royal Holloway, University of London. The UCLM and the IBMCP researchers constitute the Associated Unit TOMAFRAN. Some figures were created with BioRender.com.

CONFLICTS OF INTEREST

The authors declare no conflicts of interest.

SUPPORTING INFORMATION

Additional Supporting Information may be found in the online version of this article.

Figure S1. Results of T0 fruits from transgenic Xantomato.

Figure S2. Variable importance projection (VIP) values of PLS-DA using the genotype of Xantomato mutations or the presence/absence of the transgene.

Figure S3. *Cs*CCD2 expression in F2 from TF x Xantomato and TF fruits.

Figure S4. Individual carotenoid results of F1, F2, and F3 fruits from the cross of Xantomato with TF.

Figure S5. Other carotenoids from F1, F3, and parental plants.

Figure S6. Subchromoplast fractionation with sucrose gradients.

Figure S7. Fruit weight and number of fruits per plant in the F3 generation.

Table S1. Primers used to genotype the *in vitro* plantlets for the presence of the transgenes.

Table S2. Primers used for qPCR analyses.

Table S3. Accumulation of individual carotenoids in F1 and parental fruits.

Table S4. Genotyping results of the F2 plants germinated *in vitro* from the cross of Tomaffron and Xantomato.

Table S5. qPCR results to calculate the number of copies of *Cs*CCD2.

REFERENCES

Ahrazem, O., Diretto, G., Argandoña, J., Rubio-Moraga, A., Julve, J.M., Orzáez, D. *et al.* (2017) Evolutionarily distinct carotenoid cleavage dioxygenases are responsible for crocetin production in Buddleja davidii. *Journal of Experimental Botany*, **68**, 4663–4677.

Ahrazem, O., Diretto, G., Rambla, J.L., Rubio-Moraga, Á., Lobato-Gómez, M., Frusciante, S. *et al.* (2022) Engineering high levels of saffron apocarotenoids in tomato. *Horticulture Research*, **9**, 1–13.

Ahrazem, O., Rubio-Moraga, A., Berman, J., Capell, T., Christou, P., Zhu, C. *et al.* (2016) The carotenoid cleavage dioxygenase CCD2 catalysing the synthesis of crocetin in spring crocuses and saffron is a plastidial enzyme. *The New Phytologist*, **209**, 650–663.

Ahrazem, O., Zhu, C., Huang, X., Rubio-Moraga, A., Capell, T., Christou, P. *et al.* (2022) Metabolic engineering of Crocin biosynthesis in Nicotiana species. *Frontiers in Plant Science*, **13**, 1–11.

Barja, M.V., Ezquerro, M., Beretta, S., Diretto, G., Florez-Sarasa, I., Feixes, E. *et al.* (2021) Several geranylgeranyl diphosphate synthase isoforms supply metabolic substrates for carotenoid biosynthesis in tomato. *The New Phytologist*, **231**, 255–272.

Bathaie, S.Z., Farajzade, A. & Hoshyar, R. (2014) A review of the chemistry and uses of crocins and crocetin, the carotenoid natural dyes in saffron, with particular emphasis on applications as colorants including their use as biological stains. *Biotechnic & Histochemistry*, **89**, 401–411.

Bino, R.J., de Vos, C.H.R., Lieberman, M., Hall, R.D., Bovy, A., Jonker, H.H. *et al.* (2005) The light-hyperresponsive high pigment-2dg mutation of tomato: alterations in the fruit metabolome. *The New Phytologist*, **166**, 427–438.

Butelli, E., Titta, L., Giorgio, M., Mock, H.P., Matros, A., Peterek, S. *et al.* (2008) Enrichment of tomato fruit with health-promoting anthocyanins by expression of select transcription factors. *Nature Biotechnology*, **26**, 1301–1308.

Cerdá-Bernad, D., Valero-Cases, E., Pastor, J.J. & Frutos, M.J. (2022) Saffron bioactives crocin, crocetin and safranal: effect on oxidative stress and mechanisms of action. *Critical Reviews in Food Science and Nutrition*, **62**, 3232–3249. Available from: https://doi.org/10.1080/10408398.2020.1864279

Chattopadhyay, T., Hazra, P., Akhtar, S., Maurya, D., Mukherjee, A. & Roy, S. (2021) Skin colour, carotenogenesis and chlorophyll degradation mutant alleles: genetic orchestration behind the fruit colour variation in tomato. *Plant Cell Reports*, **40**, 767–782.

D'Ambrosio, C., Stigliani, A.L. & Giorio, G. (2011) Overexpression of CrtR-b2 (carotene beta hydroxylase 2) from S. Lycopersicum L. differentially affects xanthophyll synthesis and accumulation in transgenic tomato plants. *Transgenic Research*, **20**, 47–60.

D'Ambrosio, C., Stigliani, A.L., Rambla, J.L., Frusciante, S., Diretto, G., Enfissi, E.M.A. *et al.* (2023) A xanthophyll-derived apocarotenoid regulates carotenogenesis in tomato chromoplasts. *Plant Science*, **328**, 111575.

Demurtas, O.C., Francisco, B., De, R., Diretto, G., Diretto, G., Ferrante, P. *et al.* (2019) ABCC transporters mediate the vacuolar accumulation of Crocins in saffron stigmas. *Plant Cell*, **31**, 2789–2804.

Demurtas, O.C., Sulli, M., Ferrante, P., Mini, P., Martí, M., Aragonés, V. *et al.* (2023) Production of saffron Apocarotenoids in Nicotiana benthamiana plants genome-edited to accumulate Zeaxanthin precursor. *Metabolites*, **13**, 729.

Drapal, M., Perez-Fons, L., Price, E.J., Amah, D., Bhattacharjee, R., Heider, B. *et al.* (2022) Datasets from harmonised metabolic phenotyping of root, tuber and banana crop. *Data Brief*, **42**, 108041.

Ellul, P., Garcia-Sogo, B., Pineda, B., Ríos, G., Roig, L.A. & Moreno, V. (2003) The ploidy level of transgenic plants in agrobacterium-mediated transformation of tomato cotyledons (*Lycopersicon esculenturn* L.Mili.)

is genotype and procedure dependent. *Theoretical and Applied Genetics*, **106**, 231–238.

Florian, R., **Benoit, G.**, **Amrit, S.** & **Kim-Anh, L.C.** (2017) mixOmics: an R package for omics feature selection and multiple data integration. *PLoS Computational Biology*, **13**, 1–14.

Fraser, P.D., **Enfissi, E.M.A.** & **Bramley, P.M.** (2009) Genetic engineering of carotenoid formation in tomato fruit and the potential application of systems and synthetic biology approaches. *Archives of Biochemistry and Biophysics*, **483**, 196–204.

Frusciante, S., **Demurtas, O.C.**, **Sulli, M.**, **Mini, P.**, **Aprea, G.**, **Diretto, G.** ***et al.*** (2022) Heterologous expression of Bixa orellana cleavage dioxygenase 4–3 drives crocin but not bixin biosynthesis. *Plant Physiology*, **188**, 1469–1482.

Frusciante, S., **Diretto, G.**, **Bruno, M.**, **Ferrante, P.**, **Pietrella, M.**, **Prado-Cabrero, A.** ***et al.*** (2014) Novel carotenoid cleavage dioxygenase catalyzes the first dedicated step in saffron crocin biosynthesis. *Proceedings of the National Academy of Sciences*, **111**, 12246–12251.

Galpaz, N., **Wang, Q.**, **Menda, N.**, **Zamir, D.** & **Hirschberg, J.** (2008) Abscisic acid deficiency in the tomato mutant high-pigment 3 leading to increased plastid number and higher fruit lycopene content. *The Plant Journal*, **53**, 717–730.

Gómez Gómez, L., **Morote, L.**, **Frusciante, S.**, **Rambla, J.L.**, **Diretto, G.**, **Niza, E.** ***et al.*** (2022) Fortification and bioaccessibility of saffron apocarotenoids in potato tubers. *Frontiers in Nutrition*, **9**, 1–15.

Hirschberg, J. (2001) Carotenoid biosynthesis in flowering plants. *Current Opinion in Plant Biology*, **4**, 210–218.

Hosseini, A., **Razavi, B.M.** & **Hosseinzadeh, H.** (2018) Pharmacokinetic properties of saffron and its active components. *European Journal of Drug Metabolism and Pharmacokinetics*, **43**, 383–390.

Huang, X., **Morote, L.**, **Zhu, C.**, **Ahrazem, O.**, **Capell, T.**, **Christou, P.** ***et al.*** (2022) The biosynthesis of non-endogenous Apocarotenoids in transgenic Nicotiana glauca. *Metabolites*, **12**, 575.

Husaini, A.M. (2014) Challenges on climate change: omics-based biology of saffron plants and organic agricultural biotechnology for sustainable saffron production. *GM Crops & Food*, **5**, 97–105.

Kachanovsky, D.E., **Filler, S.**, **Isaacson, T.** & **Hirschberg, J.** (2012) Epistasis in tomato color mutations involves regulation of phytoene synthase 1 expression by cis-carotenoids. *Proceedings of the National Academy of Sciences of the United States of America*, **109**, 19021–19026.

Karniel, U., **Koch, A.**, **Zamir, D.** & **Hirschberg, J.** (2020) Development of zeaxanthin-rich tomato fruit through genetic manipulations of carotenoid biosynthesis. *Plant Biotechnology Journal*, **18**, 2292–2303.

Lê, S., **Josse, J.** & **Husson, F.** (2008) FactoMineR: an R package for multivariate analysis. *Journal of Statistical Software*, **25**, 1–18.

Levin, I., **Frankel, P.**, **Gilboa, N.**, **Tanny, S.** & **Lalazar, A.** (2003) The tomato dark green mutation is a novel allele of the tomato homolog of the DEETIOLATED1 gene. *Theoretical and Applied Genetics*, **106**, 454–460.

Li, Y., **Wang, H.**, **Zhang, Y.** & **Martin, C.** (2018) Can the world's favorite fruit, tomato, provide an effective biosynthetic chassis for high-value metabolites? *Plant Cell Reports*, **37**, 1443–1450.

López, A.J., **Frusciante, S.**, **Niza, E.**, **Ahrazem, O.**, **Rubio-Moraga, Á.**, **Diretto, G.** ***et al.*** (2021) A new glycosyltransferase enzyme from family 91, ugt91p3, is responsible for the final glucosylation step of crocins in saffron (Crocus sativus l.). *International Journal of Molecular Sciences*, **22**, 1–17.

Martí, M., **Diretto, G.**, **Aragonés, V.**, **Frusciante, S.**, **Ahrazem, O.**, **Gómez-Gómez, L.** ***et al.*** (2020) Efficient production of saffron crocins and picrocrocin in Nicotiana benthamiana using a virus-driven system. *Metabolic Engineering*, **61**, 238–250.

Mitra, S., **Estrada-Tejedor, R.**, **Volke, D.C.**, **Phillips, M.A.**, **Gershenzon, J.** & **Wright, L.P.** (2021) Negative regulation of plastidial isoprenoid pathway by herbivore-induced β-cyclocitral in Arabidopsis thaliana. *Proceedings of the National Academy of Sciences of the United States of America*, **118**, 1–12.

Moraga, A.R., **Nohales, P.F.**, **Pérez, J.A.F.** & **Gómez-Gómez, L.** (2004) Glucosylation of the saffron apocarotenoid crocetin by a glucosyltransferase isolated from Crocus sativus stigmas. *Planta*, **219**, 955–966.

Moraga, Á.R., **Rambla, J.L.**, **Ahrazem, O.**, **Granell, A.** & **Gómez-Gómez, L.** (2009) Metabolite and target transcript analyses during Crocus sativus stigma development. *Phytochemistry*, **70**, 1009–1016.

Morote, L., **Lobato-Gómez, M.**, **Ahrazem, O.**, **Argandoña, J.**, **Olmedilla-Alonso, B.**, **López-Jiménez, A.J.** ***et al.*** (2023) Crocins-rich tomato extracts showed enhanced protective effects in vitro. *Journal of Functional Foods*, **101**, 1–8.

Morote, L., **Rubio-Moraga, Á.**, **López Jiménez, A.J.**, **Aragonés, V.**, **Diretto, G.**, **Demurtas, O.C.** ***et al.*** (2023) Verbascum species as a new source of saffron apocarotenoids and molecular tools for the biotechnological production of crocins and picrocrocin. *The Plant Journal*, **14**, 1–15.

Mustilli, A.C., **Fenzi, F.**, **Ciliento, R.**, **Alfano, F.** & **Bowler, C.** (1999) Phenotype of the tomato high pigment-2 mutant is caused by a mutation in the tomato homolog of DEETIOLATED1. *Plant Cell*, **11**, 145–157.

Nogueira, M., **Berry, H.**, **Nohl, R.**, **Klompmaker, M.**, **Holden, A.** & **Fraser, P.** (2016) Subchromoplast fractionation protocol for different Solanaceae fruit species. *Bio-Protocol*, **6**, e1861.

Nogueira, M., **Enfissi, E.M.A.**, **Martínez Valenzuela, M.E.**, **Menard, G.N.**, **Driller, R.L.**, **Eastmond, P.J.** ***et al.*** (2017) Engineering of tomato for the sustainable production of ketocarotenoids and its evaluation in aquaculture feed. *Proceedings of the National Academy of Sciences of the United States of America*, **114**, 10876–10881.

Nogueira, M., **Mora, L.**, **Enfissi, E.M.A.**, **Bramley, P.M.** & **Fraser, P.D.** (2013) Subchromoplast sequestration of carotenoids affects regulatory mechanisms in tomato lines expressing different carotenoid gene combinations. *Plant Cell*, **25**, 4560–4579.

Perez-Fons, L., **Drapal, M.**, **Nogueira, M.**, **Berry, H.M.**, **Almeida, J.**, **Enfissi, E.M.A.** ***et al.*** (2022) *Metabolomic approaches for the characterization of carotenoid metabolic engineering in planta*, 1st edition. Amsterdam, The Netherlands: Elsevier Inc.

Polturak, G., **Grossman, N.**, **Vela-Corcia, D.**, **Dong, Y.**, **Nudel, A.**, **Pliner, M.** ***et al.*** (2017) Engineered gray mold resistance, antioxidant capacity, and pigmentation in betalain-producing crops and ornamentals. *Proceedings of the National Academy of Sciences of the United States of America*, **114**, 9062–9067.

Rameshrad, M., **Razavi, B.M.** & **Hosseinzadeh, H.** (2018) Saffron and its derivatives, crocin, crocetin and safranal: a patent review. *Expert Opinion on Therapeutic Patents*, **28**, 147–165.

Rao Davuluri, G., **van Tuinen, A.**, **Fraser, P.D.**, **Manfredonia, A.**, **Newman, R.**, **Burgess, D.** ***et al.*** (2005) Fruit-specific RNAi-mediated suppression of DET1 enhances carotenoid and flavonoid content in tomatoes. *Nature Biotechnology*, **23**, 1–7.

Rodriguez-Concepcion, M., **Avalos, J.**, **Bonet, M.L.**, **Boronat, A.**, **Gomez-Gomez, L.**, **Hornero-Mendez, D.** ***et al.*** (2018) A global perspective on carotenoids: metabolism, biotechnology, and benefits for nutrition and health. *Progress in Lipid Research*, **70**, 62–93.

Ronen, G., **Carmel-Goren, L.**, **Zamir, D.** & **Hirschberg, J.** (2000) An alternative pathway to β-carotene formation in plant chromoplasts discovered by map-based cloning of Beta and old-gold color mutations in tomato. *Proceedings of the National Academy of Sciences of the United States of America*, **97**, 11102–11107.

Winterhalter, P. & **Straubinger, M.** (2000) Saffron—renewed interest in an ancient spice. *Food Review International*, **16**, 39–59.

Xu, Z., **Xu, Z.**, **Pu, X.** ***et al.*** (2020) Tandem gene duplications drive divergent evolution of caffeine and crocin biosynthetic pathways in plants. *BMC Biology*, **18**, 1–14.

Yoo, H.J., **Chung, M.Y.**, **Lee, H.A.**, **Lee, S.B.**, **Grandillo, S.**, **Giovannoni, J.J.** ***et al.*** (2023) Natural overexpression of CAROTENOID CLEAVAGE DIOXYGENASE 4 in tomato alters carotenoid flux. *Plant Physiology*, **192**, 1289–1306.

Zheng, X., **Mi, J.**, **Balakrishna, A.**, **Liew, K.X.**, **Ablazov, A.**, **Sougrat, R.** ***et al.*** (2022) Gardenia carotenoid cleavage dioxygenase 4a is an efficient tool for biotechnological production of crocins in green and non-green plant tissues. *Plant Biotechnology Journal*, **20**, 2202–2216.

Zheng, X., **Mi, J.**, **Deng, X.** & **Al-Babili, S.** (2021) LC-MS-based profiling provides new insights into Apocarotenoid biosynthesis and modifications in citrus fruits. *Journal of Agricultural and Food Chemistry*, **69**, 1842–1851.